Available online at www.sciencedirect.com
ScienceDirect
Biochimica et Biophysica Acta 1768 (2007) 3206–3215
Biochimica et Biophysica Acta
BBA
www.elsevier.com/locate/bbamem

Probing the structure of the Ff bacteriophage major coat protein transmembrane helix dimer by solution NMR

Yanqiu Wu, Steve C.C. Shih, Natalie K. Goto *

Department of Chemistry, University of Ottawa, 10 Marie Curie, Ottawa, ON, K1N 6N5 Canada

Received 1 July 2007; received in revised form 8 August 2007; accepted 9 August 2007
Available online 24 August 2007

Abstract

The transmembrane (TM) segment of the major coat protein from Ff bacteriophage has been extensively studied as an example of dimerization in detergent and lipid bilayer systems. However, almost all the information regarding this interaction has been gained through mutagenesis studies, with little direct structural information being available. To this end solution NMR has the potential to provide new insights into structure of the dimer. In order to evaluate the utility of this approach we have studied a selectively ^{15}N-labeled peptide containing the TM segment of MCP (MCP_{TM}) by solution NMR. This peptide was found to give rise to detergent concentration-dependent spectra that were assigned to monomeric and dimeric forms. The standard free energy of this interaction in SDS was estimated from these spectra and found to be consistent with weak but specific dimerization. In addition, similar spectra could be obtained in β-octyl glucoside with intermolecular paramagnetic relaxation experiments demonstrating a parallel arrangement of TM helices in the dimer. In both detergents backbone chemical shift differences between monomeric and dimeric forms of MCP_{TM} showed that the largest changes occur around its GXXXG motif. The resulting structural model is consistent with observations made for MCP mutants previously characterized in biological membranes, opening the door to detailed structural characterization of this form of MCP. These results also have general implications for the study of weakly interacting TM segments by solution NMR since the use of similar sample conditions should allow structural data to be accessed for oligomeric states from a wide range systems that undergo biologically relevant but weak associations in the membrane.

Keywords: Solution NMR; Transmembrane peptide; Helix–helix interaction; Ff bacteriophage major coat protein; Paramagnetic relaxation enhancement

1. Introduction

The ability of transmembrane (TM) helices to interact once integrated into lipid bilayers underlies the formation of oligomeric membrane protein assemblies with biologically important functional properties. One of the most well-characterized structural motifs that can drive TM helix association is known as the GXXXG motif [1,2], so named for the occurrence of two glycine residues separated by three amino acids in the primary sequence. Originally identified in the transmembrane segment of glycophorin A (GpA), the association of GXXXG motif-containing TM helices has since been demonstrated for a number of different proteins that use self-association to modulate protein function, such as integrin αIIb [3], a vacuolating toxin [4,5], and the pro-apoptotic protein BNip3 [6,7]. Self-association of TM segments via this motif has been shown to occur in a variety of environments, including biological membranes [4,6,8,9], model bilayers [10,11] and detergent solutions [7,12–16]. Mutational analyses performed in these systems have shown that the strength of these interactions depends in part on the complementarity of residues flanking the glycine residues, with bulky, hydrophobic residues often being favored at these sites.

Abbreviations: TM, transmembrane; GpA, glycophorin A; MCP, major coat protein; SDS, sodium dodecyl sulfate; β-OG, β-octyl glucoside; TFA, trifluoroacetic acid; HPLC, high performance liquid chromatography; BCA, bicinchoninic acid; BSA, bovine serum albumin; MTSL, 1-oxyl-2,2,5,5-tetramethyl-Δ^3-pyrrolin-3-yl methyl methanethiosulfonate; CD, circular dichroism; HSQC, heteronuclear single quantum coherence; TOCSY, total correlation spectroscopy; NOESY, nuclear Overhauser enhancement spectroscopy; PRE, paramagnetic relaxation enhancement; AIR, ambiguous interaction restraints; C_8E_5, *n*-octyl pentaoxyethylene glycol monoether

* Corresponding author. Tel.: +1 613 562 5800x6918; fax: +1 613 562 5170.
E-mail address: ngoto@uottawa.ca (N.K. Goto).

0005-2736/$ - see front matter © 2007 Elsevier B.V. All rights reserved.
doi:10.1016/j.bbamem.2007.08.010

While the GXXXG motif is highly over-represented in databases of TM segment sequences [2], only two of these proteins have had high-resolution structures determined for the dimer: GpA [11,17] and BNip3 [18]. For both proteins, structures were determined using NMR spectroscopy on peptides solubilized in detergent or bicelle solutions, with solid-state NMR also being used to elucidate the GpA dimer structure in a lipid bilayer environment. These structures show that the two Gly residues fall on one side of the TM helix to create a flat surface that facilitates close approach of the interacting partner, while residues flanking this glycine surface engage in packing interactions that stabilize the association. Inter-helical hydrogen bonding between polar side chains was observed in both structures, providing the basis for the exceptionally high dimerization affinity for these proteins. This level of molecular detail has helped to improve understanding of protein–protein interactions in membranes, particularly for strong interactions that are likely to be constitutive in vivo. However, many biologically relevant TM helix interactions are weaker, providing a mechanism for modulation of function through reversible self-association.

One well-characterized example of a TM helix dimer shown to weakly associate via the GXXXG motif is that of the major coat protein (MCP) from the Ff group of filamentous bacteriophage. Encoded by gene VIII, ~2700 copies of this 50 residue protein encapsulate the single-stranded circular DNA genome, comprising the most abundant component of the phage particle [19]. After infection of *Escherichia coli*, MCP from disassembled phage, as well as newly synthesized gene products, are stably integrated into the bacterial inner membrane from where they are then incorporated into progeny phage. During this storage period in the cell membrane, MCP dimerizes via an interaction that differs from the staggered arrangement of subunits found in the phage particle [20,21]. Therefore in order for phage to properly assemble, this dimer interface must be disrupted to allow formation of the phage-bound oligomer. When this is not possible, as is the case when irreversible dimerization is introduced via cysteine cross-links, phage assembly cannot occur. It has been suggested that reversible self-interaction in the membrane may facilitate phage assembly by allowing higher affinity interactions between the MCP oligomer and actively extruding phage DNA while at the same time excluding lipids from this assembly domain [21]. Therefore in order to fulfill this dual role, MCP would have to participate in self-interactions in the cell membrane that are strong enough to facilitate phage assembly without interfering with the MCP interactions critical for packaging in the phage particle. It has been shown that a GXXXG motif is important for this interaction [8,16,22], although a high-resolution structure has not yet been determined for this dimer.

Structure elucidation of weakly interacting TM segments such as the MCP dimer can be complicated by difficulties in finding sample conditions that allow the observation of intermolecular interactions. Crystallographic methods are at a particular disadvantage in this respect since crystallization of these samples is hindered by their inherent heterogeneity. This is not necessarily a problem for solution NMR however, which has the potential to provide insight into these assemblies so long as a significant proportion of the population is in the oligomeric form. Through the use of high protein:detergent ratios that increase the effective concentration of protein in the detergent phase it should be possible to obtain NMR spectra that primarily reflect the higher order oligomeric state. In order to evaluate the utility of this approach we have studied the weakly interacting MCP dimer in detergent solutions by solution NMR. Using chemical shift mapping and intermolecular paramagnetic relaxation experiments with selectively ^{15}N-labeled MCP TM peptide, we found that a predominantly dimeric state could be observed in SDS or β-OG detergents. A structural model constructed from this data suggests that this interaction occurs via a right-handed coiled-coil structure as has been observed for other GXXXG motif containing proteins. Comparison with data from previous mutagenesis studies suggests that this dimer is similar to the structure occurring in biological membranes. Therefore, the use of sample conditions with low relative detergent concentrations has the potential to be generally useful for the study of oligomeric structures involving TM segments that exhibit a weak but specific interaction.

2. Materials and methods

2.1. Peptide synthesis

MCP_{TM} and its mutants were synthesized using standard Fmoc chemistry on a PerSeptive Biosystems Pioneer peptide synthesizer as previously described [16] using the standard (45 min) cycle. The *N*-[(dimethylamino)-1*H*-1,2,3-triazolo [4,5-b]pyridine-1-ylmethylene]-*N*-methylmethanaminium hexafluorophosphate *N*-oxide (HATU, PerSeptive Biosystems)/*N*,*N*-diisopropylethylamine (DIEA, Sigma-Aldrich) activator pair was used with a 4-fold excess of Fmoc-protected amino acid. A low load Fmoc-PAL-PEG-PS resin (0.17 mmol/g, PerSeptive Biosystems) was used to produce an amidated C-terminus. After synthesis, peptides were cleaved from the resin with a cocktail of 88% trifluoroacetic acid (TFA), 5% phenol, 5% ultrapure water and 2% triisopropylsilane (TIPS). The cleaved peptides were precipitated using ice-cold diethyl ether and then filtered though a Buchner filter funnel and then dried under vacuum. For selectively ^{15}N-labeled peptides the same procedure was used except that Fmoc-protected ^{15}N-labeled amino acids (Cambridge Isotope Laboratories) were used instead of the unlabeled amino acids at specific sites in the amino acid sequence.

2.2. Peptide purification

The crude peptide was resuspended in 10% acetonitrile, 0.01% trifluoroacetic acid (TFA) in water for purification by reverse-phase HPLC on a C4 semi-preparative column (Waters, 15-μm spherical silica, 300 Å pore size with C4 bonded phase) using a 2%/min acetonitrile gradient in 0.01% (v/v) aqueous TFA and elution monitored by absorbance at 215 nm. The desired peptide product comprised the major species of the crude product and eluted at ~70% acetonitrile. The purified product was lyophilized and electrospray ionization mass spectrometry was performed by the University of Ottawa Mass Spectrometry Centre to confirm the identity of the purified sample. Analytical HPLC chromatography on a C4 column (Waters, 5-μm spherical silica, 100-Å pore sizes with C4 bonded phase) was used to confirm the purity of the peptide which was generally found to be >98%.

2.3. Peptide concentration determination

Peptide concentrations were determined in duplicate using the bicinchoninic acid (BCA) protein assay (Pierce Biotech) and bovine serum albumin (BSA) protein standards made from a BSA stock solution (Pierce Biotech). Relative

concentrations were also measured in duplicate using UV absorbance of the peptide in 6 M guanidium chloride, 20 mM phosphate buffer, pH 6.5 at 280 nm with the theoretical extinction coefficient determined from the primary sequence (ε280=8250 M^{-1} cm^{-1} for MCP_{TM} and V33C and 6970 M^{-1} cm^{-1} for Y21C) [23] and were found to be within 10% of the values obtained with BCA assay.

2.4. Preparation of spin-labeled peptides

Mutants containing a cysteine residue at a specific site were synthesized and purified as described above. Peptides were dissolved in water and which was then incubated overnight with a 10-fold molar excess of the sulfhydril-reactive nitroxide spin label 1-oxyl-2,2,5,5-tetramethyl-Δ^3-pyrrolin-3-yl methyl methanethiosulfonate (MTSL; Toronto Research Chemicals) at pH ~8. Excess spin label was removed by a subsequent purification step using HPLC as described above and the identity of the final spin-labeled peptide confirmed by electrospray ionization mass spectroscopy. When required, reduction of the nitroxide spin label was achieved by addition of a 2- to 3-fold molar excess of ascorbic acid and incubation at 37 °C for 1 h.

2.5. NMR spectroscopy

Approximately 0.1–0.5 mM of lyophilized selectively ^{15}N-labeled peptide was dissolved in 10% D2O with various concentrations of SDS or β-octyl glucoside (OG) detergents while maintaining the pH at 5.5. The sensitivity enhanced version of the 2D ^{1}H–^{15}N HSQC experiments [24] with a 1.7-s recycle delay were recorded at 37 °C on the 500-MHz Varian INOVA or at 41 °C on the 500-MHz Bruker Avance spectrometer in the University of Ottawa Faculty of Science NMR Facility. Spectra were processed and analyzed using NMRPipe [25] and NMRView [26] with resolution enhancement (90° shifted sine-bell squared function in both dimensions). Backbone amide proton and nitrogen chemical shift assignments of the MCP_{TM} peptide in detergent micelles were obtained by comparison with published assignments [27] in combination with ^{15}N-HSQC-TOCSY and ^{15}N-HSQC-NOESY spectra [28]. Average backbone amide chemical shift differences ($\Delta\delta$) between monomeric and dimeric forms were calculated according to the formula $\Delta\delta=((\Delta\delta_{HN})^2+(\Delta\delta_N/5)^2)^{0.5}$ where $\Delta\delta_{HN}$ and $\Delta\delta_N$ are the chemical shift differences between monomeric and dimeric species for the amide proton and nitrogen atoms, respectively. The fraction of the population in the dimeric form was determined from peak volumes measured using the nlinLS function in NMRPipe.

2.6. Circular dichroism (CD) spectroscopy

Far-UV circular dichroism (CD) spectra were recorded on a Jasco-810 instrument with 50 and 100 μM MCP_{TM} samples using solvent conditions identical to those used for NMR experiments. Four to eight scans were performed from 250 to 200 nm with a step resolution of 0.2 nm, a speed of 20 nm/min, a bandwidth of 1.0 nm, and response time of 2 s using a 0.1-mm path-length quartz cuvette.

2.7. Modeling

Two helices with side chains in lowest energy rotameric configurations were docked using the chemical shift and paramagnetic relaxation enhancement (PRE) data determined in β-OG with rigid body docking protocols in HADDOCK [29]. Chemical shift perturbations determined in β-octylglucoside that were larger than the average shift difference were used to generate AIR (ambiguous interaction restraints) restraints, with surface neighbors of the active residues taken as passive residues. PRE data were converted into three categories of distance restraints similar to previous studies [30,31]. Specifically, I_{para}/I_{dia} ratios <15% had a range of 2–15 Å, between 15 and 85%, a range of 2–21 Å; and >85%, a range of 2–29 Å. Dihedral angle restraints ($\phi=-65°$ and $\psi=-40°\pm2.5$ and ±5.0 respectively) were imposed with a force constant of 50 to maintain the helix structure. Non-cystallographic symmetry (NCS) restraints were imposed with a force constant value of 2 while electrostatic energy terms were not used. Default settings for all other parameters were employed and the 10 lowest energy structures from the 100 structures generated from the rigid body docking protocol were taken as the final model ensemble.

3. Results

3.1. Peptide design

It has been shown that synthetic peptides containing just the transmembrane segment of MCP are able to dimerize in detergents [16,32]. The ability to generate these peptides via chemical synthesis opens the door to the introduction of specific labels. To simplify the characterization of the oligomeric state of MCP by NMR spectroscopy, a peptide corresponding to residues 21 to 48 of wild-type MCP was synthesized with ^{15}N-labeled amino acids incorporated into Gly, Ala, Leu and Val residues for a total of 12 ^{15}N-labeled sites (MCP_{TM}, labeled residues highlighted in grey in Fig. 1). This choice of labeling allowed the peptides to be synthesized at a relatively low cost using commercially available Fmoc-protected amino acids, and also ensured that the heteronuclear spectroscopic probe would be distributed along the length of the dimerization interface. In order to improve the amide chemical shift dispersion for the central hydrophobic part of the peptide and increase the number of labeled sites, Leu was substituted for Met28 and Val31, the latter of which was also expected to increase dimerization affinity [32]. Three non-native lysine residues were also included at the N-terminus, and the C-terminus was amidated to improve peptide solubility without significantly affecting the ability of peptide to dimerize as has been previously established [16].

3.2. MCP_{TM} forms weakly associated dimers in SDS micelles

It has been shown that the appearance of ^{1}H–^{15}N HSQC spectra of selectively ^{15}N-labeled MCP_{TM} in high concentra-

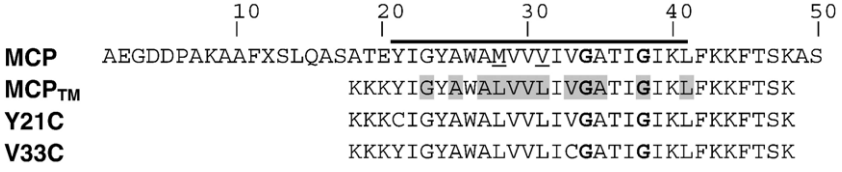

Fig. 1. Primary sequence of MCP from Ff bacteriophage and peptides used in the current study. The part of the sequence corresponding to the transmembrane helix is indicated by the line [58], with the glycine residues in the GXXXG motif shown in bold. Backbone amide nitrogen atoms were labeled with ^{15}N for all amino acids highlighted in grey in MCP_{TM}. Underlined residues in MCP are changed to Leu in all peptide sequences. Amino acid numbering for synthetic peptides after the N-terminal lysine tag followed that of the native MCP sequence starting from Y21.

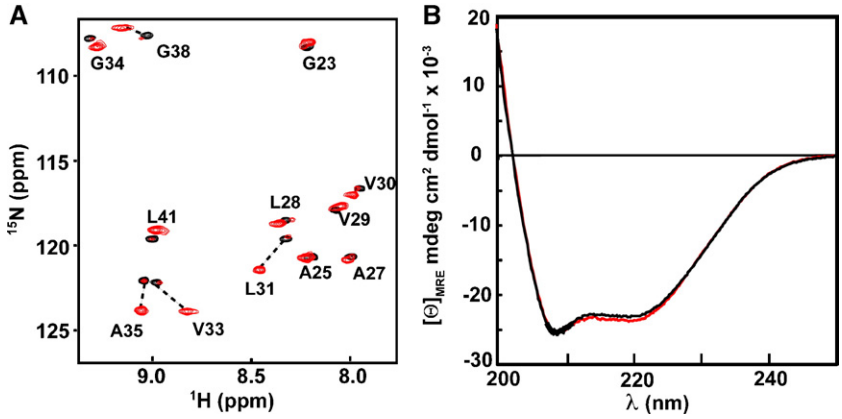

Fig. 2. (A) Assigned NMR and (B) CD spectra of MCP_{TM} in SDS. CD and NMR spectra were acquired on the same sample of 0.1 mM MCP_{TM} in either 15 mM (red spectra) or 100 mM (black spectra) SDS, pH 5.5 at 37 °C.

tions of SDS gives rise to the expected 12 peaks with a chemical shift dispersion characteristic of an α-helical structure [16]. However, as the detergent concentration is decreased, a distinct set of peaks arise in the spectrum that are broader than those obtained at high concentration, suggestive of a higher molecular weight species in slow exchange with the lower molecular weight species. The relative proportion of this species increases as the molar ratio of protein:detergent is further increased and becomes the major species when the number of SDS micelles approaches the number of MCP_{TM} molecules (Fig. 2A, red spectrum). This change in the spectrum was reversible, since adding detergent or peptide to samples showing one set of peaks in the NMR spectrum would allow peaks corresponding to the alternate species to be obtained.

To determine whether this change in the NMR spectrum was related to a change in the secondary structure of MCP_{TM}, CD spectra were recorded for MCP_{TM} under conditions that predominantly favored one species. As shown in Fig. 2B, the CD spectrum of MCP_{TM} showed minima at 208 and 222 nm, characteristic of the high degree of α-helical secondary structure that has previously been demonstrated for the MCP TM segment [8]. Highly similar CD spectra were obtained at both high and low SDS concentrations demonstrating that the differences in the NMR spectra were not due to a change in the secondary structure content of MCP_{TM}, paralleling observations with the strong TM helix dimer formed by GpA [33]. Instead, this reversible detergent concentration-dependent change in the spectrum likely reflects a change in the MCP_{TM} oligomerization state, with the broad species in the high protein:detergent sample corresponding to the dimeric state.

Comparison of MCP_{TM} spectra with previously published spectra on the full-length protein in SDS [27] showed that they are highly similar, as would be expected due to the absence of interactions between the TM segment and other regions of

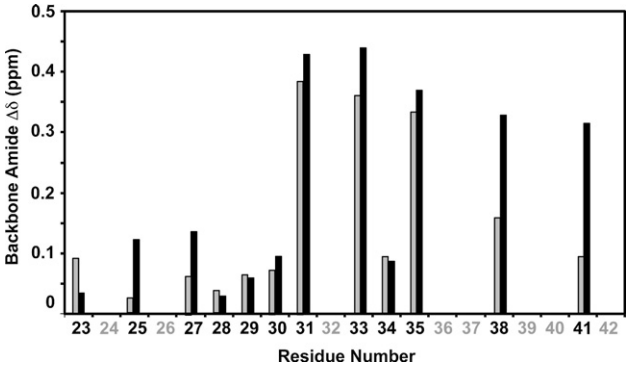

Fig. 3. Average backbone ^{1}H and ^{15}N amide chemical shift differences (Δδ) between MCP_{TM} monomer and dimer peaks in SDS (grey bars) and β-OG (black bars) as determined from spectra in Figs. 2A and 5A, respectively. Residue numbers for regions of the sequence containing ^{15}N-labeled backbone amide atoms are indicated in black lettering, with non-labeled residues in grey.

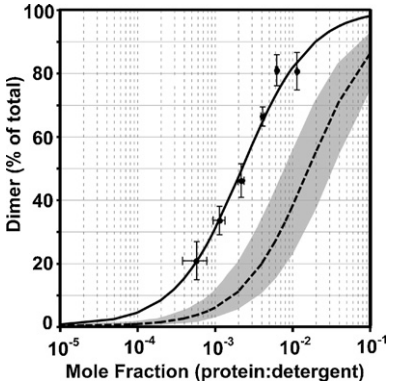

Fig. 4. MCP_{TM} association in SDS micelles. Each point represents the population of dimer as a percent of the total protein concentration as determined from peak volumes measured for each species in the NMR spectrum recorded at 41 °C with the indicated mole fraction of protein to micellar detergent. The continuous line represents the calculated distribution for a monomer–dimer equilibrium with a standard free energy of association of −3.8 kcal/mol. The distribution predicted for MCP_{TM} if dimer formation is a result of random partitioning into a limited number of micelles is represented by the dashed line, as calculated by the Poisson distribution for MCP_{TM} in micelles composed of 60 SDS molecules. The range of distributions that would occur in this case if the number of detergent molecules comprising the micelle was increased or decreased by 50% is shaded in grey.

MCP. When used in combination with ^{15}N-HSQC-TOCSY and ^{15}N-HSQC-NOESY spectra it was possible to assign the twelve ^{15}N-labeled residues for both forms. Regions of the peptide that were experiencing a significant change in local chemical environment between the two species were then identified by measuring the average difference in backbone amide chemical shifts. As shown in Fig. 3, significant shift differences were observed in the central portion of the TM helix for Leu31, Val33 and Ala 35. All residues outside of this central portion showed shifts that were at or below the average shift difference, suggesting that the two species in the NMR spectrum are associating via the central part of the TM helix as expected from previous studies. In particular, amino acids at positions 31 and 35 have been shown to be important for the interaction, with Cys mutants made at these sites being able to form cross-links in biological membranes [20,21]. Therefore these chemical shift differences support the assignment of these two species as the monomeric and dimeric forms of MCP_{TM}.

In order to estimate the affinity of MCP_{TM} dimerization, a series of ^{1}H–^{15}N HSQC spectra were acquired at a range of protein:detergent ratios, and peak volumes determined for the five residues showing distinct shifts in the monomeric and dimeric species. These volumes were used to determine the percent population of MCP_{TM} that was in the dimeric form, and the average of these values was then plotted as a function of the molar ratio of protein to micellar detergent (Fig. 4). It has previously been shown for proteins that are confined to the micellar phase that the standard free energy of association (ΔG_x^0) for a monomer–dimer equilibrium (i.e., 2 monomers (dimer)), can be determined according to:

$$\Delta G_{\text{app}} = \Delta G_x^o + RT\ \ln([\text{micellar SDS}]\gamma_{\text{SDS}}) \tag{1}$$

where (ΔG_{app}) is the apparent free energy of association, [micellar SDS] is the total concentration of SDS minus the critical micelle concentration (cmc) and γ_{SDS} is the activity coefficient accounting for deviations from thermodynamically ideal solution conditions [34]. The apparent association energy is related to the apparent dissociation constant (K_{app}) by:

$$\Delta G_{\text{app}} = RT\ \ln K_{\text{app}} \tag{2}$$

with

$$K_{\text{app}} = \frac{[M]^2[\text{micellar SDS}]\gamma_{\text{SDS}}}{[D]} \tag{3}$$

where $[D]$ and $[M]$ are the molar concentrations of peptide in dimeric and monomeric form, respectively. Hence the population of peptide that is in dimeric form (f_{d}) can be related to the apparent dissociation constant by:

$$f_{\text{d}} = \frac{[D]}{[D]+[M]} = \frac{[M]}{\frac{K_{\text{app}}}{[\text{micellar SDS}]\gamma_{\text{SDS}}}+[M]}. \tag{4}$$

Using these relationships and assuming that $\gamma_{\text{SDS}}=1$, the dimer populations determined from the NMR spectra could be fit to a distribution curve for a monomer–dimer equilibrium with a standard interaction energy of −3.8 kcal/mol. This is significantly weaker than the free energy of association determined for GpA in SDS which was estimated to be −5.5 kcal mol^{-1} when ideal solution behavior was assumed [33]. In addition, SDS micelles would not be expected to exhibit ideal behavior at the concentrations used in our study, and hence this likely represents an overestimate of the energy of the standard interaction energy [34]. While the magnitude of this effect is not known, if $\gamma_{\text{SDS}}=0.5$ (which would correspond to the value predicted by the Debye–Huckel limiting law for a 300 mM monovalent salt solution), this would reduce the standard interaction energy to −3.4 kcal mol^{-1}. A similar degree of overestimation has been suggested to arise for GpA in SDS [34], although further experimentation would be required to definitively quantitate the impact of non-ideality in these systems.

While the association of the MCP_{TM} dimer in SDS is weak, it is stronger than would be predicted if it was solely due to a

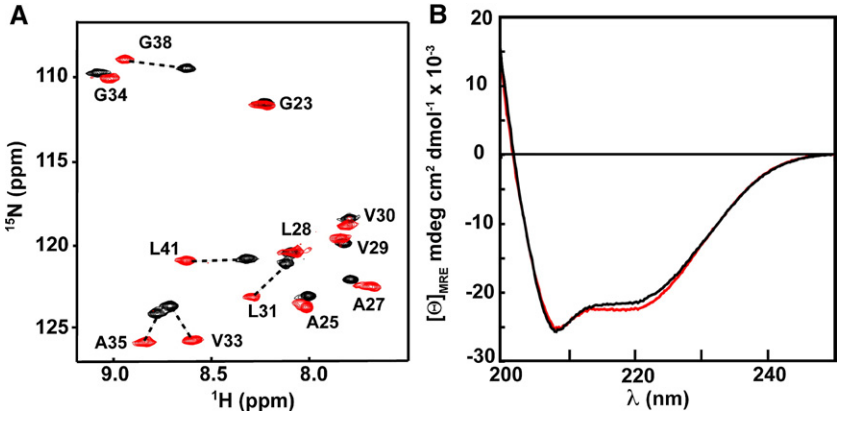

Fig. 5. (A) Assigned NMR and (B) CD spectra of MCP_{TM} in β-OG. CD and NMR spectra were acquired on the same sample of 0.1 mM MCP_{TM} in either 25 mM (red spectra) or 100 mM (black spectra) β-OG, pH 5.5 at 37 °C.

random distribution of MCP_{TM} in the micelles. It has previously been shown that when there is no preferential interaction, the frequency of occurrence of two peptides in a single micelle can be described by a statistical model according to the Poisson distribution [35]. Assuming that a micelle can only incorporate one or two peptides, the percent of the population predicted to appear as a dimer is given by:

$$\%\text{Dimer} = \frac{x}{x+1} \times 100\% \quad (5)$$

where x is the molar ratio of proteins to micelles. As shown in Fig. 4, for a micelle aggregation number of 60 this model predicts significantly lower populations of dimer than observed in our experiment. This remains the case even when larger or smaller aggregation numbers are assumed, further supporting the idea that MCP_{TM} forms weak but specific dimers in SDS.

3.3. MCP_{TM} dimerization in β-OG

Since our results indicated that MCP_{TM} undergoes a specific self-interaction in SDS, it should be possible to observe this dimer in other detergent environments that may be more favorable for solution NMR. β-OG was chosen for this part of the study since it is frequently characterized as a non-denaturing detergent [36] and it readily forms micelles of a size that is compatible with solution NMR [37]. As shown in Fig. 5, MCP_{TM} dissolved in β-OG showed two different sets of peaks depending on the concentration of detergent used. Similar to the spectrum of the dimer in SDS, the set of peaks obtained at low β-OG concentrations was broad in comparison to those obtained at the high detergent concentration sample. CD spectroscopy also confirmed that these spectral differences were not due to differences in secondary structure content, with a high degree of helicity being present in both types of samples (Fig. 5B). The pattern of average backbone amide chemical shift differences between the two species was also comparable to those obtained in SDS (Fig. 3), suggesting that the two species correspond to monomeric and dimeric MCP_{TM}. Assuming a cmc of ~20 mM [37], slightly higher ratios of protein:micellar detergent appeared to be required to obtain significant proportions of dimer species. Unfortunately it was not possible to straightforwardly quantitate the strength of this interaction in β-OG as was done for SDS, as peaks tended to move and broaden when significant levels of both species were present, suggesting that the rate of interconversion between the two species was intermediate to fast on the NMR time-scale. Nonetheless, the fact that a predominantly dimeric species could be obtained at a protein:micellar detergent molar ratio of ~0.02 (Fig. 5A) is consistent with a preferential self-association for MCP_{TM} in β-OG micelles.

Since oligomerization of MCP_{TM} in β-OG has not previously been studied, we wanted to confirm that the two spectra observed in our studies corresponded to different oligomeric states of MCP_{TM}. For this purpose a variant of MCP_{TM} was synthesized with Val33 replaced by Cys (V33C) to allow derivatization with the sulfhydryl-reactive nitroxide spin label MTSL. By mixing this spin-labeled peptide with the selectively ^{15}N-labeled MCP_{TM}, it was possible to monitor the effect of the spin label on the proton linewidths in the MCP_{TM} spectrum. As shown in Fig. 6A, a sample displaying the putative dimer spectrum (red) was mixed with 0.8 molar equivalents of spin-labeled peptide to yield a spectrum showing significant loss of signal intensity (yellow spectrum). The largest degree of intensity reduction was observed in the central portion of the peptide, as would be expected from the central location of the Cys33 in the TM segment. Since the only source of paramagnetic relaxation was attached to a peptide that had no ^{15}N isotope label itself, this effect was intermolecular in origin, confirming an oligomeric state for this species. In addition, the peak intensities could be recovered by addition of β-OG to a concentration of 100 mM, demonstrating that the lower protein:detergent spectrum corresponds to a primarily monomeric species. These data provide direct evidence that the two different spectra obtained in β-OG

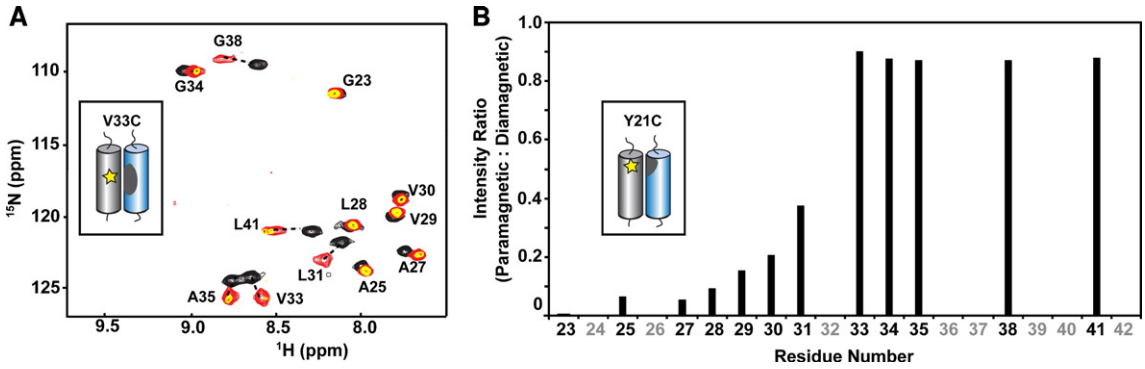

Fig. 6. Paramagnetic spin relaxation suggests MCP_{TM} forms parallel dimers in β-OG. Experiments were run using selectively ^{15}N-labeled MCP_{TM} (shown in the inset schematic diagram as a blue cylinder) mixed with the indicated MTSL-derivatized mutant with no ^{15}N label (grey cylinder with MTSL represented by the yellow star) in order to look for intermolecular paramagnetic broadening in the ^{15}N-labeled peptide (grey patch in the blue cylinder). (A) ^{1}H–^{15}N HSQC spectra of 0.3 mM selectively ^{15}N-labeled MCP_{TM} in 30 mM β-OG either alone (red spectrum) or mixed with 0.2 mM of MTSL-derivatized V33C (yellow spectrum) plotted at the same level. The intensity of the broadened peaks was recovered by adding β-OG to this same sample to a concentration of 100 mM (black spectrum). (B) Intermolecular paramagnetic broadening between 0.25 mM MCP_{TM} and an equimolar amount of MTSL-labeled Y21C in 30 mM β-OG at 37 °C. Intensity ratios for peaks from spectra before and after reduction of the nitroxide radical by ascorbic acid are plotted as a function of residue number.

reflect different oligomerization states, likely following a monomer–dimer equilibrium as was observed in SDS.

To unequivocally determine whether self-association in β-OG was occurring between parallel versus anti-parallel peptides another variant of MCP_{TM} was made with the Cys introduced closer to the N-terminus of the peptide (Y21C). Similar to the previous experiment, an equimolar mixture of the MTSL-labeled peptide was mixed with the selectively ^{15}N-labeled MCP_{TM} in conditions favoring the oligomeric spectrum and found to give rise to broadening for a subset of residues. Reduction of the nitroxide spin label with ascorbic acid allowed the intensity of the PRE-broadened peaks to be normalized with respect to their intensities in the absence of PRE. As shown in Fig. 6B, the degree of broadening was most significant in the N-terminal region of the peptide, with the effect becoming gradually less pronounced for residues approaching the central portion of the TM helix. Since the radius of influence for the MTSL nitroxide radical is ~15 Å, these data demonstrate that the oligomeric form of MCP_{TM} in β-OG must contain a parallel arrangement of TM helices. Taken together, the β-OG data show similar features to the dimer that has been characterized in SDS, as would be expected for these weakly interacting, but specifically associated peptides.

4. Discussion

MCP from filamentous bacteriophage has been a major focus of investigation for several decades in a range of studies reflecting the diverse functional roles that are performed by this simple polypeptide. It has frequently been studied as a model monotopic membrane protein [38–43], as a critical component of bacteriophage assembly [32,44–47], and as a TM helix dimer [8,22,48–51]. In the current work we are interested in its ability to reversibly associate via the widely occurring GXXXG motif and in the potential utility of solution NMR approaches to provide biologically relevant structural information on the dimeric form. In fact, MCP was one of the first TM helix-containing proteins to be studied by solution NMR in detergent micelles and was shown at that time to give rise to two peaks for each TM segment resonance [52]. Although this peak doubling was originally attributed to a dimeric form of the protein, because those spectra were acquired at high protein:SDS detergent ratios, the relevance of this form was subsequently called into question [53]. Since the experimental conditions were thought to force multiple copies of the MCP into a single micelle, the observed change in local chemical environment was attributed to non-specific effects. Nonetheless, it has since been demonstrated that MCP undergoes preferential self-association in biological membranes via its TM segment [20,21], raising the possibility that the two species originally observed in the NMR spectrum for MCP dissolved in SDS arose from this specific interaction.

In the current work we have provided evidence that the transmembrane segment from MCP undergoes specific self-association in detergents. In particular, we observed peak doubling for peptides comprised of the TM segment of MCP with the relative proportion of species being affected by the concentration of detergent, as has been shown for strongly interacting TM segments such as GpA. The helical content of these two species is identical, while the peak linewidths are not, suggesting that the two species correspond to monomeric and dimeric forms of MCP_{TM}. Quantitation of dimer populations from these spectra showed that more dimer was present than would be expected if this population solely arose from the random incorporation of two peptides in a single micelle (Fig. 4). In addition, the standard energy of interaction for MCP_{TM} in SDS is stronger than those determined for TM segments from receptor tyrosine kinases (e.g., the ErbB receptor in the polar detergent C_8E_5 [54] and the cck4 receptor in the zwitterionic detergent C14 betaine [35]) and is similar in magnitude to the erythropoietin receptor TM segment in C_8E_5 [55]. Since the standard interaction energy is detergent-specific, containing contributions from detergent–detergent and detergent–peptide interactions, this energy will likely be different for the full-length MCP in biological membranes. However, the magnitude of this energy determined for the truncated, lysine-tagged peptide in SDS indicates that the different species obtained at high versus low protein:detergent ratios most likely arise from a specific self-interaction and are not a non-specific consequence of two peptides being confined to one micelle.

If the self-association of MCP_{TM} in SDS is the result of a specific interaction then it should be possible to observe in other detergents, as was the case in our study. In fact, similar detergent concentration-dependent changes in the NMR spectrum could be obtained in β-OG (Fig. 3), with the shifts reflecting changes

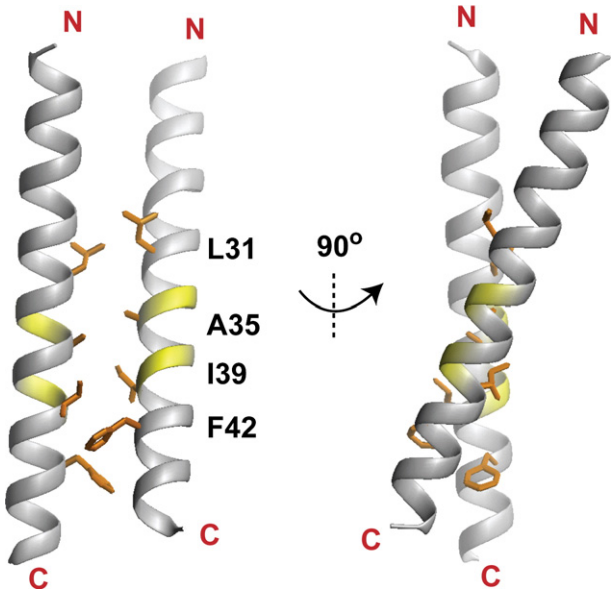

Fig. 7. Model of the MCP dimer. Two idealized helices corresponding to MCP_{TM} were subjected to rigid-body docking with ambiguously defined restraints according to the chemical shift differences between the monomer and dimer and PRE-based distance restraints from MTSL-labeled Y21C. Parts of the helices corresponding to the Gly residues from the GXXXG motif are indicated in yellow, with interfacial sidechains shown and labeled. Only the model with the lowest energy from the ensemble is shown, however, the 10 structures with lowest energy are all highly similar, with a heavy atom R.M.S.D. of 1.3 Å ± 0.6 Å to the mean structure.

in oligomeric state as established by intermolecular PRE (Fig. 6). Evaluation of the shift differences between the two forms showed the same pattern of shifts as those obtained in SDS, although the magnitude was larger for G38 and L41 in β-OG. The shift changes for these residues may have been smaller in SDS due to the interaction that has been shown to occur between the detergent sulfate headgroups and lysine residues close to the C-terminus (i.e., K40, K43, K44) [56]. This could counteract the charge of the lysine sidechains and may even facilitate dimerization by reducing electrostatic repulsion between these groups across the dimer. Consistent with this idea, dimerization of MCP is promoted by the use of high pH solutions, which would be expected to reduce this electrostatic repulsion [57]. A similar interaction may also occur with the negatively charged headgroup phase of the bacterial inner membrane [58]. In contrast, dimerization in β-OG would bring these charges in close proximity without a shielding headgroup environment, leading to a larger change in the electrostatic field experienced by the spins in this region of the peptide. Therefore in the case of MCP_{TM}, the use of β-OG as a membrane mimetic may allow greater sensitivity to changes in the local chemical environment that occur upon dimerization.

It is useful to note that the PRE experiments in our study utilized extremely high protein:detergent ratios that could be anticipated to force more than two peptides into a single micelle. For example, assuming an aggregation number of 90, 0.5 mM MCP_{TM} dissolved in 30 mM β-OG should give rise to a significant population of micelles with 4–5 peptides incorporated. Although the impact of these conditions on the physical properties of the micelle is not known, it appears that this did not change the spectrum of the dimer itself or give rise to additional peaks. Nonetheless, the PRE results provide evidence that more than two peptides were incorporated into a significant proportion of the micelles, since a small but uniform degree of broadening also occurred in the central and C-terminal regions of the protein (Fig. 6B). This is consistent with a sub-population of spin-labeled peptide being in a random orientation relative to the ^{15}N-labeled dimeric species, which would be expected if more than two peptides were present in a single micelle. Therefore, even under conditions where a micelle is highly loaded with peptide, the specificity of the MCP_{TM} interaction dominates the NMR spectrum.

Although we have established that specific TM helix interactions for MCP_{TM} can be retained in detergent solutions compatible with NMR, a high-resolution structure of MCP_{TM} will require a biosynthetic version that would allow uniform incorporation of isotope label. Nonetheless, even with a limited number of spectroscopic probes, unique insights into the structure of the MCP_{TM} dimer can be obtained. In our study, the backbone amide chemical shift data show that the amide groups of Leu31, Val33 and Ala35 experience a significant change in local chemical environment upon dimerization. These shift changes suggest that these residues are either in, or proximal to the dimer interface. Residues that display a small change in backbone amide chemical shifts (e.g., Val32, Gly34) are less likely to be involved in the interaction although it is not possible to rule them out since the environment of a hydrophobic micelle interior may not be very chemically distinct from a hydrophobic interaction interface.

Using the limited chemicals shifts from our study, it is possible to create a model for the MCP_{TM} dimer structure with HADDOCK, a docking program designed to account for the ambiguity in the interpretation of this type of data [29]. As shown in Fig. 7, when used in conjunction with distance restraints obtained from the PRE data from MTSL-labeled Y21C, this approach generates a MCP_{TM} dimer model with a right-handed coiled coil as would be expected for a GXXXG motif. The resulting dimer shows Ala35 and Leu31 localized to the dimer interface and Val33 well outside of this interface, which is consistent with cross-linking results obtained in biological membranes [20,21]. In addition, Gly38 interacts with the Ile39 across the dimer, two residues that have also been implicated in dimer formation in detergents [8,32]. However, the average helix crossing angle in the ensemble is $-27\pm1°$, which is smaller than the $-35°$ to $-40°$ crossing angle for GpA and BNip3 [11,17,18]. In addition, in those structures both glycine residues in the GXXXG motif participate in packing interactions while in our model Gly34 does not seem to be interfacial. While we cannot rule out the possibility that these differences may be resolved when more complete chemical shift data sets can be acquired, our model is not necessarily inconsistent with the report that the G34I mutant of MCP disrupts dimerization [32], since it is possible that this glycine residue is close enough to the dimerization interface that introduction of a bulky residue could destabilize the interaction. Moreover, alternative models that maximize the involvement of the Gly face in the dimer interface do not necessarily provide a better explanation of experimental results. For example, in a previous model where the glycine faces pack against each other with a helix crossing angle of $-40°$, Ala35 and Val31 are peripheral to the dimer interface, separated by a distance that does not appear to be consistent with the experimental cross-linking between Cys mutants observed in vivo [8]. Overall, the differences observed between models illustrate the potential for variation to arise in GXXXG motif-containing TM peptides and highlight the importance of gaining more insight into the range of structures that can be adopted by this motif in the membrane. This information will also help to explain why the presence of the GXXXG motif alone does not necessarily ensure that the helix will self-associate [59], improving our ability to predict dimerization sequences.

In summary we have demonstrated that the TM segment of MCP forms dimers in detergent micelles that have features that are similar to those found in biological membranes. Even under conditions that lead to high protein loading of detergent micelles the specific dimerization interface is maintained while non-specific interactions are not observed. This has general implications for the study of weakly interacting TM segments since the structures of other weakly associated membrane proteins should also be accessible by solution NMR through the use of sample conditions with low relative detergent concentrations.

Acknowledgements

We are grateful to Dr. Tito Scaiano for providing access to his CD spectrometer, Dr. John Pezacki for his assistance with peptide synthesis and Dr. Charles Deber for his input and encouragement during the initiation of this project. This work was supported by a Research Innovation Award from the Research Corporation and grants from the Natural Sciences and Engineering Research Council (NSERC) and the Canadian Foundation for Innovation (CFI).

References

[1] M.A. Lemmon, H.R. Treutlein, P.D. Adams, A.T. Brunger, D.M. Engelman, A dimerization motif for transmembrane alpha-helices, Nat. Struct. Biol. 1 (1994) 157–163.
[2] A. Senes, M. Gerstein, D.M. Engelman, Statistical analysis of amino acid patterns in transmembrane helices: the GxxxG motif occurs frequently and in association with beta-branched residues at neighboring positions, J. Mol. Biol. 296 (2000) 921–936.
[3] A.W. Partridge, S.C. Liu, S. Kim, J.U. Bowie, M.H. Ginsberg, Transmembrane domain helix packing stabilizes integrin αIIb beta 3 in the low affinity state, J. Biol. Chem. 280 (2005) 7294–7300.
[4] M.S. McClain, et al., Essential role of a GXXXG motif for membrane channel formation by *Helicobacter pylori* vacuolating toxin, J. Biol. Chem. 278 (2003) 12101–12108.
[5] S. Kim, A.K. Chamberlain, J.U. Bowie, Membrane channel structure of *Helicobacter pylori* vacuolating toxin: role of multiple GXXXG motifs in cylindrical channels, Proc. Natl. Acad. Sci. U. S. A. 101 (2004) 5988–5991.
[6] E.S. Sulistijo, T.M. Jaszewski, K.R. MacKenzie, Sequence-specific dimerization of the transmembrane domain of the "BH3-only" protein BNIP3 in membranes and detergent, J. Biol. Chem. 278 (2003) 51950–51956.
[7] E.S. Sulistijo, K.R. MacKenzie, Sequence dependence of BNIP3 transmembrane domain dimerization implicates side-chain hydrogen bonding and a tandem GxxxG motif in specific helix–helix interactions, J. Mol. Biol. 364 (2006) 974–990.
[8] R.A. Melnyk, S. Kim, A.R. Curran, D.M. Engelman, J.U. Bowie, C.M. Deber, The affinity of GXXXG motifs in transmembrane helix–helix interactions is modulated by long-range communication, J. Biol. Chem. 279 (2004) 16591–16597.
[9] W.P. Russ, D.M. Engelman, The GxxxG motif: a framework for transmembrane helix–helix association, J. Mol. Biol. 296 (2000) 911–919.
[10] B.D. Adair, D.M. Engelman, Glycophorin-A helical transmembrane domains dimerize in phospholipid-bilayers — a resonance energy-transfer study, Biochemistry 33 (1994) 5539–5544.
[11] S.O. Smith, D. Song, S. Shekar, M. Groesbeek, M. Ziliox, S. Aimoto, Structure of the transmembrane dimer interface of glycophorin A in membrane bilayers, Biochemistry 40 (2001) 6553–6558.
[12] E. Arbely, Z. Granot, I. Kass, J. Orly, I.T. Arkin, A trimerizing GxxxG motif is uniquely inserted in the severe acute respiratory syndrome (SARS) coronavirus spike protein transmembrane domain, Biochemistry 45 (2006) 11349–11356.
[13] J.D. Lear, A.L. Stouffer, H. Gratkowski, V. Nanda, W.F. DeGrado, Association of a model transmembrane peptide containing Gly in a heptad sequence motif, Biophys. J. 87 (2004) 3421–3429.
[14] M.A. Lemmon, et al., Glycophorin-A dimerization is driven by specific interactions between transmembrane alpha-helices, J. Biol. Chem. 267 (1992) 7683–7689.
[15] K.G. Fleming, D.M. Engelman, Specificity in transmembrane helix–helix interactions can define a hierarchy of stability for sequence variants, Proc. Natl. Acad. Sci. U. S. A. 98 (2001) 14340–14344.
[16] R.A. Melnyk, A.W. Partridge, J. Yip, Y.Q. Wu, N.K. Goto, C.M. Deber, Polar residue tagging of transmembrane peptides, Biopolymers 71 (2003) 675–685.
[17] K.R. MacKenzie, J.H. Prestegard, D.M. Engelman, A transmembrane helix dimer: structure and implications, Science 276 (1997) 131–133.
[18] E.V. Bocharov, et al., Unique dimeric structure of BNip3 transmembrane domain suggests membrane permeabilization as a cell death trigger, J. Biol. Chem. 282 (2007) 16256–16266.
[19] D.A. Marvin, Filamentous phage structure, infection and assembly, Curr. Opin. Struct. Biol. 8 (1998) 150–158.
[20] N.G. Haigh, R.E. Webster, The major coat protein of filamentous bacteriophage f1 specifically pairs in the bacterial cytoplasmic membrane, J. Mol. Biol. 279 (1998) 19–29.
[21] C. Nagler, G. Nagler, A. Kuhn, Cysteine residues in the transmembrane regions of M13 procoat protein suggest that oligomeric coat proteins assemble onto phage progeny, J. Bacteriol. 189 (2007) 2897–2905.
[22] R.M. Johnson, A. Rath, R.A. Melnyk, C.M. Deber, Lipid solvation effects contribute to the affinity of Gly-XXX-Gly motif-mediated helix–helix interactions, Biochemistry 45 (2006) 8507–8515.
[23] H. Edelhoch, Spectroscopic determination of tryptophan and tyrosine in proteins, Biochemistry 6 (1967) 1948–1954.
[24] L.E. Kay, P. Keifer, T. Saarinen, Pure absorption gradient enhanced heteronuclear single quantum correlation spectroscopy with improved sensitivity, J. Am. Chem. Soc. 114 (1992) 10663–10665.
[25] F. Delaglio, S. Grzesiek, G.W. Vuister, G. Zhu, J. Pfeifer, A. Bax, NmrPipe—a multidimensional spectral processing system based on Unix pipes, J. Biomol. NMR 6 (1995) 277–293.
[26] B.A. Johnson, R.A. Blevins, NMRView—a computer-program for the visualization and analysis of NMR data, J. Biomol. NMR 4 (1994) 603–614.
[27] G.D. Henry, B.D. Sykes, Assignment of amide 1H and 15N NMR resonances in detergent-solubilized M13 coat protein—a model for the coat protein dimer, Biochemistry 31 (1992) 5284–5297.
[28] D. Marion, et al., Overcoming the overlap problem in the assignment of ^{1}H-NMR spectra of larger proteins by use of 3-dimensional heteronuclear ^{1}H-^{15}N Hartmann-Hahn multiple quantum coherence and nuclear Overhauser multiple quantum coherence spectroscopy—application to interleukin-1-beta, Biochemistry 28 (1989) 6150–6156.
[29] C. Dominguez, R. Boelens, A. Bonvin, HADDOCK: a protein–protein docking approach based on biochemical or biophysical information, J. Am. Chem. Soc. 125 (2003) 1731–1737.
[30] B.Y. Liang, J.H. Bushweller, L.K. Tamm, Site-directed parallel spin-labeling and paramagnetic relaxation enhancement in structure determination of membrane proteins by solution NMR spectroscopy, J. Am. Chem. Soc. 128 (2006) 4389–4397.
[31] P. Teriete, C.M. Franzin, J. Choi, F.M. Marassi, Structure of the Na, K-ATPase regulatory protein FXYD1 in micelles, Biochemistry 46 (2007) 6774–6783.
[32] R.A. Melnyk, A.W. Partridge, C.M. Deber, Transmembrane domain mediated self-assembly of major coat protein subunits from Ff bacteriophage, J. Mol. Biol. 315 (2002) 63–72.
[33] L.E. Fisher, D.M. Engelman, J.N. Sturgis, Detergents modulate dimerization but not helicity, of the glycophorin A transmembrane domain, J. Mol. Biol. 293 (1999) 639–651.
[34] K.G. Fleming, Standardizing the free energy change of transmembrane helix–helix interactions, J. Mol. Biol. 323 (2002) 563–571.
[35] F.J. Kobus, K.G. Fleming, The GXXXG-containing transmembrane domain of the CCK4 oncogene does not encode preferential self-interactions, Biochemistry 44 (2005) 1464–1470.
[36] A.A. Seddon, P. Curnow, P.J. Booth, Membrane proteins, lipids and detergents: not just a soap opera, Biochim. Biophys. Acta 1666 (2004) 105–117.
[37] K. Kameyama, T. Takagi, Micellar properties of octylglucoside in aqueous-solutions, J. Colloid Interface Sci. 137 (1990) 1–10.
[38] F.M. Marassi, A. Ramamoorthy, S.J. Opella, Complete resolution of the solid-state NMR spectrum of a uniformly ^{15}N-labeled membrane protein in phospholipid bilayers, Proc. Natl. Acad. Sci. U. S. A. 94 (1997) 8551–8556.
[39] F.C.L. Almeida, S.J. Opella, f_d Coat protein structure in membrane

environments: structural dynamics of the loop between the hydrophobic trans-membrane helix and the amphipathic in-plane helix, J. Mol. Biol. 270 (1997) 481–495.
[40] P.V. Nazarov, R.B.M. Koehorst, W.L. Vos, V.V. Apanasovich, M.A. Hemminga, FRET study of membrane proteins: determination of the tilt and orientation of the N-terminal domain of M13 major coat protein, Biophys. J. 92 (2007) 1296–1305.
[41] P.V. Nazarov, R.B.M. Koehorst, W.L. Vos, V.V. Apanasovich, M.A. Hemminga, FRET study of membrane proteins: simulation-based fitting for analysis of membrane protein embedment and association, Biophys. J. 91 (2006) 454–466.
[42] D. Stopar, R.B. Spruijt, C. Wolfs, M.A. Hemminga, Protein–lipid interactions of bacteriophage M13 major coat protein, Biochim. Biophys. Acta 1611 (2003) 5–15.
[43] C.T.K. Yuen, A.R. Davidson, C.M. Deber, Role of aromatic residues at the lipid–water interface in micelle-bound bacteriophage M13 major coat protein, Biochemistry 39 (2000) 16155–16162.
[44] K.A. Williams, et al., Packing of coat protein amphipathic and transmembrane helices in filamentous bacteriophage-M13 — role of small residues in protein ooligomerization, J. Mol. Biol. 252 (1995) 6–14.
[45] C.M. Deber, Z.M. Li, C. Joensson, M. Glibowicka, G.Y. Xu, Transmembrane region of wild-type and mutant M13 coat proteins — conformational role of beta-branched residues, J. Biol. Chem. (1992) 5296–5300.
[46] R.B. Spruijt, C. Wolfs, M.A. Hemminga, Membrane assembly of M13 major coat protein: evidence for a structural adaptation in the hinge region and a tilted transmembrane domain, Biochemistry 43 (2004) 13972–13980.
[47] R. Jelinek, A. Ramamoorthy, S.J. Opella, High-resolution three-dimensional solid-state NMR spectroscopy of a uniformly ^{15}N-labeled protein, J. Am. Chem. Soc. 117 (1995) 12348–12349.
[48] C. Wang, C.M. Deber, Peptide mimics of the M13 coat protein transmembrane segment — retention of helix–helix interaction motifs, J. Biol. Chem. 275 (2000) 16155–16159.
[49] C.M. Deber, A.R. Khan, Z.M. Li, C. Joensson, M. Glibowicka, J. Wang, Val→Ala mutations selectively alter helix–helix packing in the transmembrane segment of phage M13 coat protein, Proc. Natl. Acad. Sci. U. S. A. 90 (1993) 11648–11652.
[50] R.M. Johnson, A. Rath, C.M. Deber, The position of the Gly-XXX-Gly motif in transmembrane segments modulates dimer affinity, Biochemistry and Cell Biology-Biochimie Et Biologie Cellulaire, vol. 84, 2006, pp. 1006–1012.
[51] J.P. Dawson, R.A. Melnyk, C.M. Deber, D.M. Engelman, Sequence context strongly modulates association of polar residues in transmembrane helices, J. Mol. Biol. 331 (2003) 255–262.
[52] G.D. Henry, B.D. Sykes, Detergent-solubilized M13 coat protein exists as an asymmetric dimer — observation of individual monomers by ^{15}N, ^{13}C and ^{1}H nuclear-magnetic-resonance spectroscopy, J. Mol. Biol. 212 (1990) 11–14.
[53] P.A. McDonnell, S.J. Opella, Effect of detergent concentration on multidimensional solution NMR-spectra of membrane-proteins in micelles, J. Magn. Reson. B. 102 (1993) 120–125.
[54] A.M. Stanley, K.G. Fleming, The transmembrane domains of ErbB receptors do not dimerize strongly in micelles, J. Mol. Biol. 347 (2005) 759–772.
[55] A.Z. Ebie, K.G. Fleming, Dimerization of the erythropoietin receptor transmembrane domain in micelles, J. Mol. Biol. 366 (2007) 517–524.
[56] C.H.M. Papavoine, R.N.H. Konings, C.W. Hilbers, F.J.M. Vandeven, Location of M13 coat protein in sodium dodecyl-sulfate micelles as determined by NMR, Biochemistry 33 (1994) 12990–12997.
[57] S. Makino, J.L. Woolford, C. Tanford, R.E. Webster, Interaction of deoxycholate and of detergents with coat protein of bacteriophage F1, J. Am. Chem. Soc. 250 (1975) 4327–4332.
[58] D. Stopar, R.B. Spruijt, M.A. Hemminga, Anchoring mechanisms of membrane-associated M13 major coat protein, Chem. Phys. Lipids 141 (2006) 83–93.
[59] D. Schneider, D.M. Engelman, Motifs of two small residues can assist but are not sufficient to mediate transmembrane helix interactions, J. Mol. Biol. 343 (2004) 799–804.